

Article

# Durability of Shape Memory Polymer Composite Laminates under Thermo-Mechanical Cycling

Fabrizio Quadrini <sup>\*</sup> , Leandro Iorio, Denise Bellisario  and Loredana Santo 

Department of Industrial Engineering, University of Rome Tor Vergata, Via del Politecnico 1, 00133 Rome, Italy; leandro.iorio@uniroma2.it (L.I.); denise.bellisario@uniroma2.it (D.B.); loredana.santo@uniroma2.it (L.S.)

\* Correspondence: fabrizio.quadrini@uniroma2.it

**Abstract:** Shape memory polymer composites (SMPCs) have been manufactured by press moulding of carbon fibre-reinforced (CFR) prepregs with SMP interlayers. SMPC laminates have been produced with different numbers of CFR plies (i.e., 2, 4, 6, and 8) and different thicknesses of the SMP interlayers (i.e., 100 and 300  $\mu\text{m}$ ) for a sum of eight combinations. Co-curing of the prepreg plies and the SMP interlayers has led to an optimal adhesion of structural and functional plies, which has been confirmed by following testing. Single thermo-mechanical cycles at increasing strains (i.e., 0.06%, 0.12%, and 0.18%) and multiple cycling have been performed to test SMPC laminate durability. Delamination and fibre cracking were not observed during testing, and laminates showed a reproducible SM behaviour after 10 consecutive thermo-mechanical cycles. SM properties have been extracted from tests in terms of residual and memory loads as well as shape fixity and shape recovery. These data may be used for comparison of the performances of the different laminates, and as a first base for designing SMPC structures. Thin laminates exhibit lower recovery loads but higher shape fixity than thick ones, but the shape recovery is very high for all the SMPCs, with an average of 98%.

**Keywords:** durability; shape memory polymer composite; composite laminate; carbon fibre-reinforced composites; thermo-mechanical cycling



**Citation:** Quadrini, F.; Iorio, L.; Bellisario, D.; Santo, L. Durability of Shape Memory Polymer Composite Laminates under Thermo-Mechanical Cycling. *J. Compos. Sci.* **2022**, *6*, 91. <https://doi.org/10.3390/jcs6030091>

Academic Editor:  
Thanasis Triantafyllou

Received: 11 February 2022

Accepted: 10 March 2022

Published: 15 March 2022

**Publisher's Note:** MDPI stays neutral with regard to jurisdictional claims in published maps and institutional affiliations.



**Copyright:** © 2022 by the authors. Licensee MDPI, Basel, Switzerland. This article is an open access article distributed under the terms and conditions of the Creative Commons Attribution (CC BY) license (<https://creativecommons.org/licenses/by/4.0/>).

## 1. Introduction

Shape memory polymer composites (SMPCs) and polymers (SMPs) have been extensively studied over the last years, and many potential uses have been found in many fields covering aerospace engineering, biomedical devices, flexible electronics, soft robotics, shape memory arrays and 4D printing [1]. Recent studies have shown the importance of molecular mobility on the definition of the SM behaviour as in the case of nanoparticle filling [2] or optimised cross-linking [3]. Carbon fibres (CFs) have an important impact on molecular mobility as well, but their use is essential for space. Despite numerous requirements that restrict the range of materials for space applications, SMPCs seem to comply with them. In fact, SMPC recovery has been tested in space under microgravity [4] with the aim of designing actuators [5], self-deployable structures [6], antennas [7], and solar sails [8]. Even if space structures may be deployed only one time, SMPC devices should withstand several memory-recovery thermo-mechanical cycles to pass the qualification stages. Therefore, durability is very important to speed up the use of SMPC structures in space, at least at a low number of cycles, as well as fully characterising SMPC functional behaviour and simplifying manufacturing procedures. In the last achievements, carbon-fibre-reinforced (CFR) SMPC laminates have been manufactured with commercial prepregs, used for aeronautical structures, and commercial SMP powders by means of conventional moulding technologies and procedures [9]. The effect of the number of plies on the SM behaviour of composite laminates was studied but single memory-recovery cycles were used.

The concept of durability is very often applied to materials and structures close to their final use; therefore, various factors, such as aging, compression and hibernation, lubricants,

UV light and thermo-mechanical cycling, are taken into account [10]. In the case of SMPCs, these factors mainly influence the resin matrix, as fibres are typically stable and inert over a wider range of loading and environmental conditions. In particular, for CFR laminates, the strong physical and thermo-mechanical stability of carbon fibres may improve durability of the organic phase. Nevertheless, SMPs may show higher sensibility to heavy duties and harsh environments than conventional polymeric matrices because of their particular functional behaviour.

In 2010, in their study on the environmental durability of fabric-reinforced SMPCs, Tandon et al. investigated the effect of simulated environmental exposure to moisture, lubrication oil and UV radiation on SM properties of some dog-bone-shaped specimens [11]. They tested low-filled composites and discussed strong SM changes after the first memory-recovery cycle, but the consideration that SM properties may change in repetitive loading conditions was valid. However, this approach has not been used by other researchers immediately. In 2015, Guo et al. evaluated the SM properties of chopped carbon fibre-reinforced trans-1,4-polyisoprene with filler content up to 13 [12] and 15 wt% [13], but cyclic loading was performed only at room temperature. In 2016, Gong et al. developed a SMPC made of a carbon fibre felt in an epoxy-based SMP [14]. They did not perform cyclic testing but, at least, the same device was used to evaluate the effect of electric heating for different heat flux densities. More recently, in 2019, Li et al. studied the shape recovery of unidirectional CFR-SMPC under bending [15]. They performed two continued free recovery cycles to evaluate the repeatability of the experiment. In fact, multiple cycles are carried out very often to assess test variability or possible training effects rather than durability. In the same year, in their study on the long-term properties of CFR-SMPCs, Jang et al. exposed 4 ply laminates to vacuum ultraviolet [16]. They performed SM tests by means of dynamic mechanical thermal analysis (DMTA) in 3 point bending configuration, but they evaluated the effect of accelerated ageing by the change in the storage modulus over exposure time. In fact, DMTA is a powerful technique for material characterisation, but it is limited in the evaluation of durability under cycling because of the very low applied displacement (only 15  $\mu\text{m}$  in that study).

The absence of durability studies by repetitive memory-recovery cycles is probably dependent on the difficulty of defining a valid testing procedure. For this reason, durability is mainly investigated with quasi-static mechanical tests before and after exposure in harsh environment (mainly UV). In fact, typical thermal chambers of universal material testing machines would apply very long times for temperature cycling with the negative effect of poor results. Moreover, the SM response of SMPCs depends on the heating rate, and thermal chambers have very high thermal inertia. As a consequence, very recent experimental studies on SMPCs continue to prefer single-cycle SM or mechanical tests, and rarely mention durability issues. In 2020, Ren et al. have studied damages in CFR-SMPC tubes made by filament winding [17]. It is not discussed if the ultimate behaviour of a SMPC structure could be influenced by preliminary memory-recovery cycles. In 2021, Margoy et al. developed SMPC actuators based on carbon resistive heating fibres and epoxy matrix for space applications. They discuss the durability of SMPC actuators in a space environment qualitatively, mainly in terms of overheating and exposure to atomic oxygen and radiations [18].

In order to obtain maximum performances from SMPCs in smart structures, it is important to perform a full assessment of their durability. SMPCs have to work under very severe conditions just for thermo-mechanical cycling and apart from possible harsh environments. Even if failure is avoided, it is possible that SM properties are partially lost during repetitive memory-recovery cycles. In order to assess this durability under thermo-mechanical cycling, it is important to set-up a robust testing procedure. The authors have already used repeated memory-recovery tests to evaluate the performances of SMPs. SMP epoxy foams for space applications were tested with different configurations under multiple recovery tests [19]. In analogy, SM properties of PET foams were assessed by applying three consecutive thermo-mechanical cycles [20]. In this study, up to 10 memory-recovery

cycles were used to test SMPC laminates. Several laminates with different numbers of plies and thicknesses of the SMP interlayers were manufactured for this aim. In the current study, single-cantilever bending tests were repeated up to 10 cycles on SMPC laminates with different numbers of CFR plies and different thicknesses of the SMP interlayers. The goal was to provide a comparison of SMP performances among different laminates in terms of durability and quantitative data for designing purposes.

## 2. Materials and Methods

SMPC laminates were manufactured by hand lamination of CFR prepregs and press moulding. Epoxy-matrix CFR prepregs for autoclave moulding (HexPly/M49/42%/CHF-3K by Hexcel) were laminated by interposing an un-cured epoxy powder with SM properties (Scotchkote 206N by 3M). The HexPly prepreg is commonly used for aeronautics; the matrix is an epoxy resin (M49), and reinforcements are in the form of a plain fabric of continuous CFs. These materials were used in previous studies to prototype several composite structures and devices [4–7]. After curing, the thermoset matrix of the CFR prepregs had very low SM properties and was easily damaged during thermo-mechanical cycling. Instead, the SMP epoxy-resin has remarkable SM properties in the shape of film or foam [4–9,19,21]. Co-curing of CFR plies and SMP interlayers under compression moulding allows the optimal joining between structural and functional layers.

### 2.1. SMPC Laminate Moulding

The SMPC samples are shown in Figure 1. Rectangular laminates, having the size of  $30 \times 100 \text{ mm}^2$ , were laminated with 2, 4, 6, and 8 CFR plies. The SMP epoxy powder was interposed between adjacent layers to have an average thickness of 100 or 300  $\mu\text{m}$ . In the end, eight different combinations of number of plies and SMP interlayer thicknesses were prototyped. Neat CFR laminates, without SMP interlayers, were not considered, because SMP testing conditions were defined, in this study, in a range where those laminates were damaged. The moulding process was operated in an aluminium mould, for each single laminate, at a temperature of 200  $^{\circ}\text{C}$ , a pressure of 70 kPa, and a holding time of 1 h. The physical data of the moulded samples are summarised in Table 1. The mean value of the thickness and its dispersion were extracted after five measurements. The average thickness dispersion was 2%, with a maximum of 4% for the sample having 6 plies and a 300  $\mu\text{m}$  interlayer. The average thickness of the CFR ply was approximately 300  $\mu\text{m}$  for the samples with a low-thickness interlayer and 400  $\mu\text{m}$  for those with high thickness. A comparable density was measured for the two classes of samples, being 1.36 and 1.34  $\text{g}/\text{cm}^3$ , respectively.

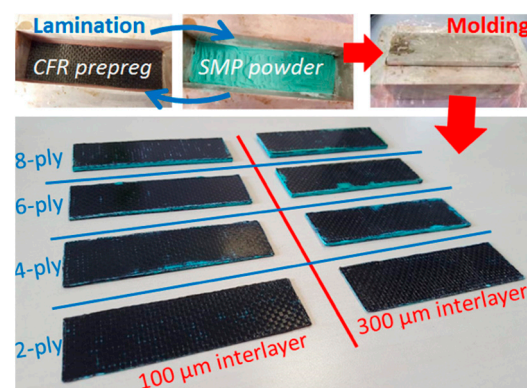


Figure 1. Samples for the durability tests.

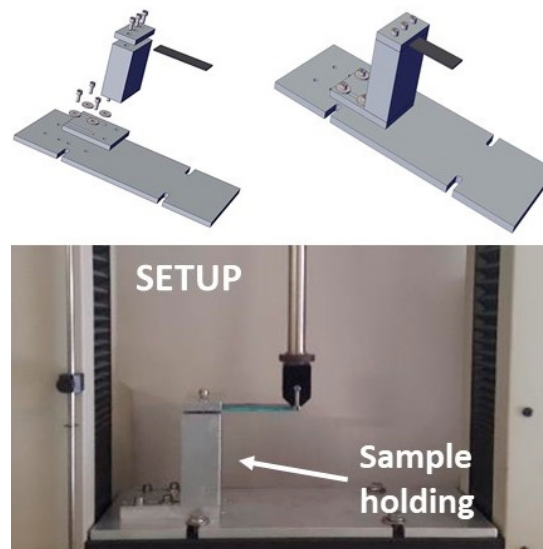
**Table 1.** Physical properties of the SMPC laminates.

SMP Interlayer Thickness ( $\mu\text{m}$ )	Number of Plies	Thickness (mm)	Weight (g)	Density ( $\text{g}/\text{cm}^3$ )
100	2	$0.52 \pm 0.01$	2.25	1.40
	4	$1.13 \pm 0.03$	4.75	1.33
	6	$1.72 \pm 0.02$	7.67	1.40
	8	$2.65 \pm 0.03$	10.87	1.31
300	2	$0.75 \pm 0.01$	3.08	1.30
	4	$1.66 \pm 0.04$	6.00	1.32
	6	$2.76 \pm 0.10$	12.10	1.38
	8	$3.53 \pm 0.07$	15.28	1.35

### 2.2. SMPC Test Device

A single-cantilever beam configuration was used for testing the SMP behaviour of the SMPC laminates.

A clamping device was built for this aim according to Figure 2.

**Figure 2.** Device and configuration for SMP testing.

This configuration allowed for reaching high displacements of the sample end, with lower values of maximum strains in comparison with other bending configurations such as dual-cantilever or 3 point. Samples were clamped from one end, along a clamping length of 20 mm, whereas a pushing rod deformed the opposite end. A span length of 80 mm resulted. The pushing rod was connected with a universal material testing machine (MTS Insight 5). In comparison with the 3 point bending configuration, the same maximum displacement was obtained with 25% of the maximum strain, but this maximum occurred at the clamping end instead of the sample middle-length. Tests were carried out up to a maximum displacement of 20 mm, depending on the laminate structure.

### 2.3. Temperature Calibration

SMP tests were performed using a hot-air gun to heat the samples during the thermo-mechanical cycles. Conventional heating chambers cannot be used because of the long set-up time and low heating rate. This heating procedure is very effective [9], but temperature data for the tests are difficult to be identified, as a temperature distribution is present along the laminate length. A calibration step is necessary for this aim. Generally, the air gun is pointed on the laminate zone where the highest strain has been applied during the memory

step. According to Figure 3, for this study, the gun tip was at 60 mm from the clamping end. Temperature calibration was performed on the thickest sample (8 plies and 300  $\mu\text{m}$  of SMP interlayer). The temperature was acquired during time in 3 different positions by type K thermocouples: close the clamping end (A), in the middle-length of the span (B), and close to the free end (C). Temperature curves are reported in Figure 4.

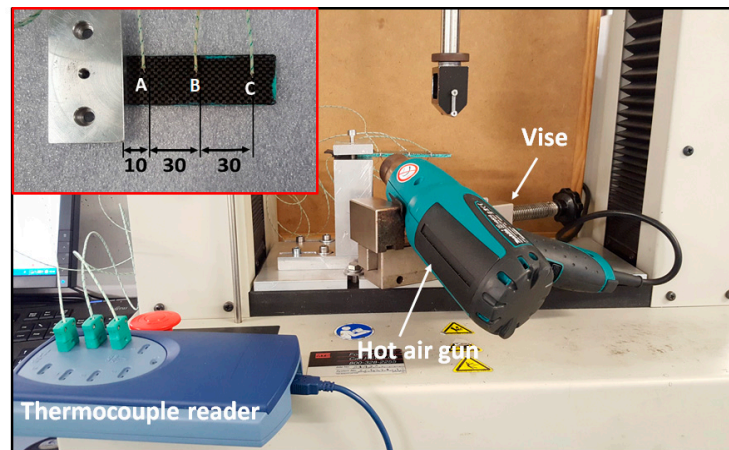


**Figure 3.** Temperature calibration for SMP testing.

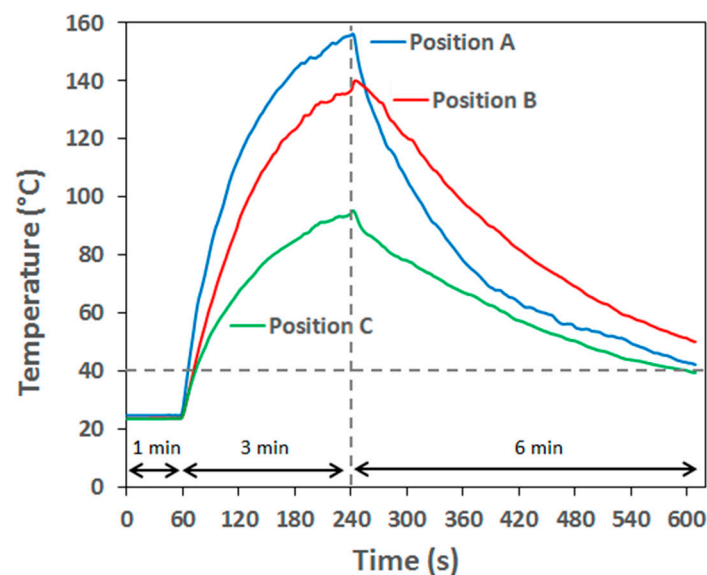


**Figure 4.** Temperature curves during calibration recorded at clamping end (A), in the middle length of the span (B) and close to the free end (C).

After 1 min, heating was applied for 3 min. As expected, the highest temperature was reached in point A, close to 160  $^{\circ}\text{C}$ , enough to allow full shape recovery of the SMPC laminates. The lowest peak-temperature was measured in the free end, close to 100  $^{\circ}\text{C}$ , which is virtually non-sufficient for full recovery, but the applied strain in the free end was zero, and shape recovery was absent. In the middle-length, a temperature close to 140  $^{\circ}\text{C}$  was reached, sufficient for shape recovery which is active from 120  $^{\circ}\text{C}$  (the glass transition temperature of the cured epoxy matrix). After 4 min, the heating was disabled and the laminate was left to cool in air. After 6 min, a temperature close to 40  $^{\circ}\text{C}$  was reached in all the laminates, far from the SMP transition temperature. At this temperature, a second heating cycle can start. In particular, the clamping end (point A) showed a faster cooling than the other two points due to the contact with the aluminium device. This is positive in the case that several thermo-mechanical cycles have to be run consecutively.

#### 2.4. The SMP Thermo-Mechanical Cycle

SMP properties are typically measured during an instrumented thermo-mechanical cycle. There are different procedures to quantify them.

Basically, SMP materials are deformed under heating by applying forces, and are cooled under the same constraints used to apply the deformation. After cooling, the constraints can be removed, but the deformed shape becomes permanent. The equilibrium shape is recovered by heating again in the absence of constraints or applied forces. Multiple memory-recovery cycles are possible if the loading stage is repeated as well.

Most of the studies on SM polymers and composites mainly quantify the SMP performances by the shape fixity,  $R_f$ , and shape recovery,  $R_r$ . These parameters refer to the ability of the material to fix the applied deformation under constraints ( $R_f$ ), thus minimising elastic recovery after constrain removal, and the ability to recover the first initial equilibrium shape ( $R_r$ ). A SMP material with 100% of both parameters is considered an ideal SMP, being able to freeze all the applied deformation of the memory step and to restore perfectly the equilibrium shape in the recovery step. In the case of SMPC, these two parameters are important as well but not sufficient to describe the full SM behaviour. First of all, due to the fibre contribution, 100% of  $R_f$  and  $R_r$  is not possible. Fibres do not show any SM property and partially damaged SM behaviour of the matrix, but fibres are added to increase material stiffness during transition and to provide higher recovery loads. Recovery loads and speeds are important data for designing SMPC actuators or deploying structures. For this reason, a new instrumented procedure has been defined to extract load values during shape recovery [21].

According to previous studies [9,21], the single thermo-mechanical cycle was carried out by the “cold deformation mode” as shown in Figure 5.

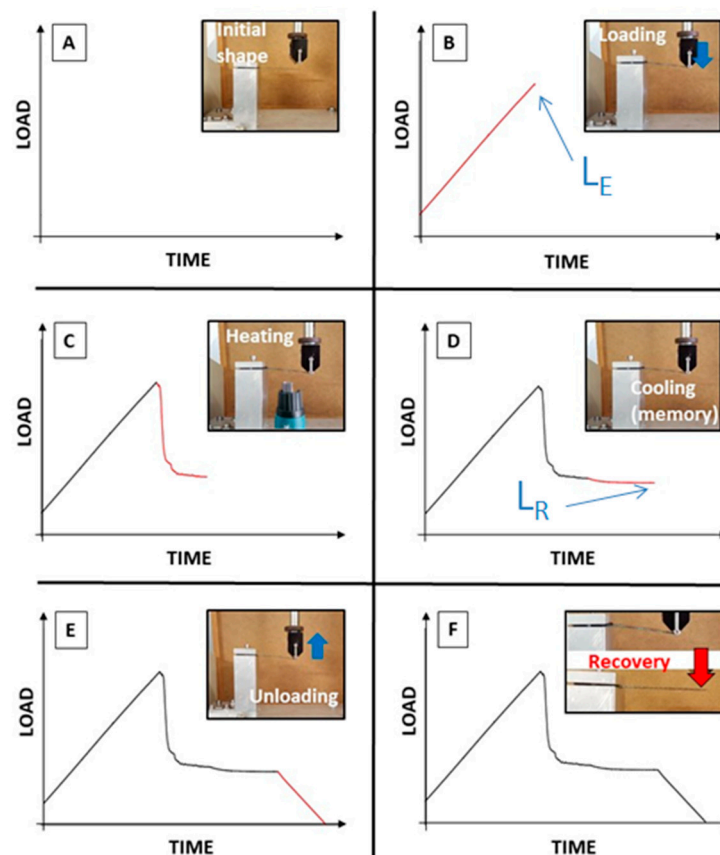


**Figure 5.** Instrumented thermo-mechanical cycle for SMPC testing. (A) equilibrium condition; (B) deformation under bending at room temperature; (C) heating stage; (D) cooling stage; (E) unloading; (F) free recovery upon heating.

In this case, the laminate starts from the equilibrium condition (A) and is deformed under bending (B) at room temperature at defined rate up to a determined maximum displacement. In the end of this stage, the maximum load is applied (elastic load =  $L_E$ ). Subsequently, the sample is heated by the hot-air gun (C). The material softens and the applied load, under fixed constraints, rapidly reduces. In the following stage, the laminate is left to cool (D). Generally, in the cooling stage, the load continues to decrease down to residual value (residual load =  $L_R$ ). The last 2 stages are those where the SMP behaviour is highlighted. In fact, a perfect elastic material, during cooling, would recover the initial stiffness up to  $L_E$ . The difference between the elastic load  $L_E$  and the residual load  $L_R$  is directly linked to the ability of the SMPC of memorising the shape (memory load =  $L_M$ ). In the end, the bending rod is moved up (E), and the residual load is zeroed by elastic recovery. The thermo-mechanical cycle is closed by heating again in absence of constraints to reach the initial equilibrium shape (F). The shape fixity is calculated by measuring the residual deformation after stage E. Instead, the shape fixity is extrapolated after measuring the residual deformation after stage F.

### 2.5. Single Thermo-Mechanical Cycles

First SMPC tests were performed with only 1 instrumented cycle but different maximum strains. In fact, because of the different thickness, laminates may behave very differently at similar displacements, and a comparison on the durability would be wrong. It is evident that the maximum attainable displacement for a thin laminate could lead to failure a thick laminate. For example, the maximum strain of 0.18% was reached in the clamped end of the thinnest laminate (2 ply, 100  $\mu\text{m}$  interlayer) at the inflection of 15 mm. The same strain is reached in the same position of the thickest laminate (8 ply, 300  $\mu\text{m}$  SMP interlayer) at the inflection of 2.2 mm. For the experimentation, 3 maximum strains were selected (i.e., 0.06%, 0.12% and 0.18%). The idea was not comparing the SM behaviour in terms of maximum allowable stresses but in the same condition of maximum strain. Table 2 reports the applied maximum inflections to the SMPC laminates for the different strains.

**Table 2.** Imposed displacement of the free end of SMPC laminates.

Interlayer	$\epsilon$ (%)	Inflection (mm)			
		2 Plies	4 Plies	6 Plies	8 Plies
100 ( $\mu\text{m}$ )	0.06	5	2.3	1.5	1
	0.12	10	4.6	3	2
	0.18	15	6.9	4.5	2.9
	0.06	3.4	1.6	0.9	0.7
300 ( $\mu\text{m}$ )	0.12	6.9	3.1	1.9	1.5
	0.18	10.3	4.7	2.8	2.2
	0.06	5	2.3	1.5	1
	0.12	10	4.6	3	2

Tests were carried out at the rate of 1 mm/min with a heating stage of 3 min and the following cooling stage of 4 min.

### 2.6. Multiple Thermo-Mechanical Cycles

Durability tests were performed on the same SMPC samples, which were already tested at increasing maximum displacement. In this case, the heating time and the cooling time were reduced to 2 min, and 10 continuous cycles were repeated for each laminate by applying the maximum strain of 0.18%. The test rate was increased to 2 mm/min to reduce the full test time, which was limited to a maximum of 3 h, in the case of the thinnest laminate.

### 3. Results

All the laminates underwent the thermo-mechanical cycles without any evidence of damages. Results from single thermo-mechanical cycles at increasing strain are reported in Figure 6.

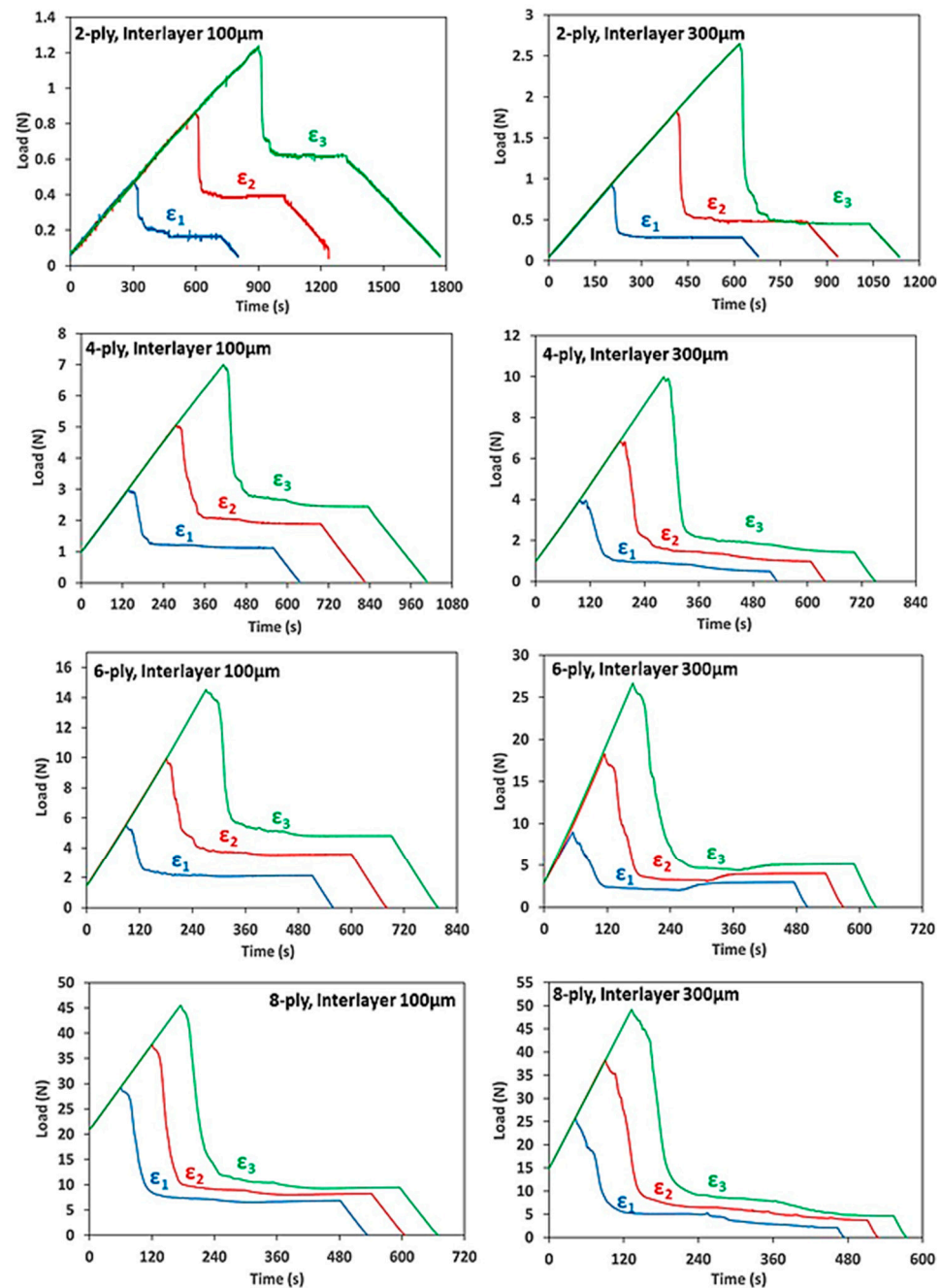


**Figure 6.** Instrumented thermo-mechanical cycle for SMP testing ( $\epsilon_1 = 0.06\%$ ,  $\epsilon_2 = 0.12\%$ ,  $\epsilon_3 = 0.18\%$ ).

The optimal superposition of the initial “cold” elastic stage shows that previous testing did not affect the laminate structure in terms of fibre crack or delamination. All the curves show the typical shape of a SMPC test with a maximum and a following plateau which is divided in two parts, one at the end of the heating range and one at the end of the cooling stage. As expected, in all the cases apart the 6 ply laminate with 300 µm SMP interlayer, a further load reduction is present from the end of the heating stage and the end of the cooling stage.

During multiple cycling, the thermo-mechanical cycles were repeated 10 times without removing the samples from the testing machine. Therefore, the shape fixity was acquired from all the cycles but the shape recovery only after the last. A typical curve is reported in Figure 7 for the case of the 4 ply laminates.

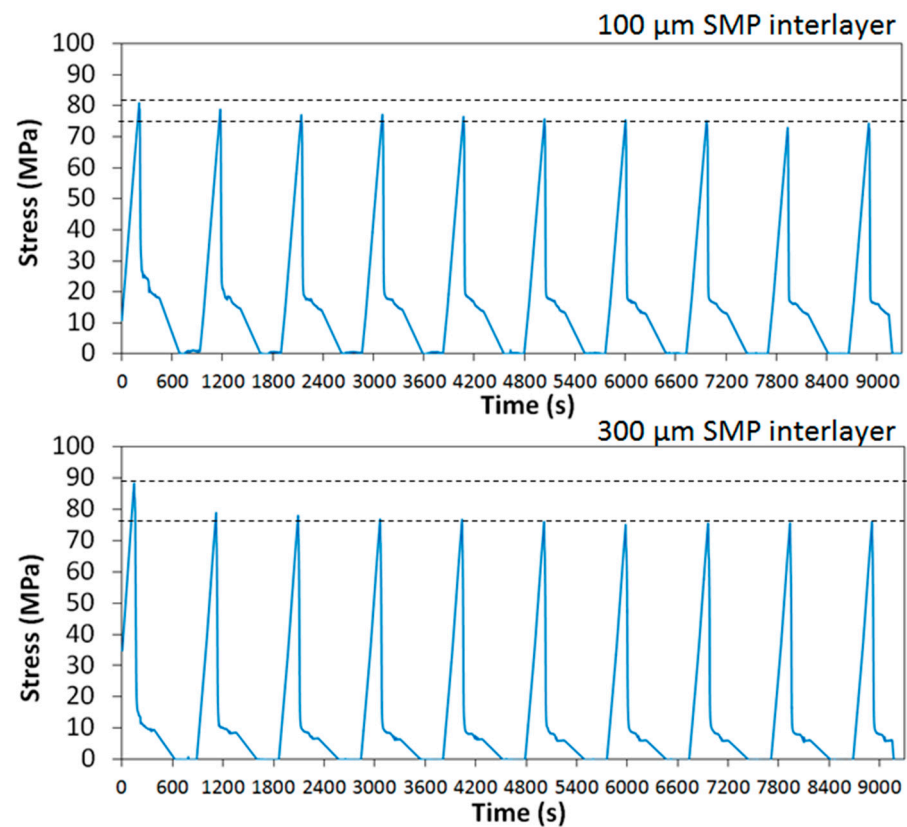


**Figure 7.** Multiple cycling on 4-ply laminates at the maximum strain.

In this case, the curve has been normalised with the bending formulas, and the stress and strain at the laminate extrados is reported. In general, all the cycles are comparable with a small difference between the first and the following. A possible training effect could be present but it should be excluded, in this case, as those laminates were already tested under single thermo-mechanical cycles at increasing strains. It is more probable that the difference of the first cycle depends on the different transient phase during heating. It is evident that thermal cycling does not affect the laminate integrity in the adopted strain range. It is not possible to identify any degradation effect by comparing the first with the last loading peaks.

#### 4. Discussion

For the first time, durability of SMPC laminates with different structures has been evaluated by an instrumented thermo-mechanical cycling even if at low cycles. Results show that these materials have very good performances which are preserved along cycles. According to expected applications of SMPCs, such as self-deployable structures for space, the observed durability is already sufficient to make functional prototypes. In fact, low cycles are requested to these structures with repetitive behaviour. The huge amount of data from this experimentation could be the first step for sizing laminates to integrate into antennas, grabbing devices of debris, solar sails, and solar panels. Tables are preferred for data representation as trends are not always clearly visible.

From a quantitative point of view, residual load ( $L_R$ ), memory load ( $L_M$ ), shape fixity ( $R_f$ ), and shape recovery ( $R_r$ ) were extracted from all the thermo-mechanical tests at

different strains (Figure 6). Reference loads were also normalised in terms of residual stress ( $\sigma_R$ ), and memory stress ( $\sigma_M$ ). These data are summarised in Table 3 for all the laminates.

**Table 3.** SM data from single thermo-mechanical cycles at increasing strain.

$\epsilon_1 = 0.06\%$	2 Plies		4 Plies		6 Plies		8 Plies	
	100 $\mu\text{m}$	300 $\mu\text{m}$						
$L_R$ (N)	0.17	0.29	1.12	0.49	2.13	2.96	6.85	2.1
$L_M$ (N)	0.31	0.64	1.89	3.5	3.43	6.04	22.48	23.69
$\sigma_R$ (MPa)	9.9	7.91	13.48	2.71	1.05	5.96	15.18	2.57
$\sigma_M$ (MPa)	15.06	17.46	22.76	19.32	27.82	12.16	49.81	28.97
$R_f$ (%)	71.33	73.19	44.45	85.14	48.5	53.26	12.02	76.34
$R_r$ (%)	93.59	96.32	98.5	100	99.25	100	100	100
$\epsilon_2 = 0.12\%$	2 Plies		4 Plies		6 Plies		8 Plies	
	100 $\mu\text{m}$	300 $\mu\text{m}$						
$L_R$ (N)	0.39	0.48	1.89	0.98	3.55	4.01	8.23	3.72
$L_M$ (N)	0.48	1.36	3.2	5.92	6.44	14.29	29.56	34.64
$\sigma_R$ (MPa)	22.72	13.09	22.63	5.41	18.43	8.07	18.24	4.55
$\sigma_M$ (MPa)	27.96	37.1	38.65	32.68	33.43	28.77	65.5	42.37
$R_f$ (%)	64.21	75.63	53.71	83.64	56.77	70.86	46.21	82.04
$R_r$ (%)	95.77	98.74	99.49	100	98.12	86.33	96.85	96.38
$\epsilon_3 = 0.18\%$	2 Plies		4 Plies		6 Plies		8 Plies	
	100 $\mu\text{m}$	300 $\mu\text{m}$						
$L_R$ (N)	0.62	0.45	2.45	1.42	4.8	5.14	9.46	4.63
$L_M$ (N)	0.62	2.2	4.56	8.57	9.74	21.56	36.03	44.58
$\sigma_R$ (MPa)	36.12	5.46	29.5	7.84	24.92	10.35	20.96	5.66
$\sigma_M$ (MPa)	36.12	66.83	54.9	55.15	50.57	43.4	79.84	54.53
$R_f$ (%)	49.57	84.57	59.02	83.76	61.18	75.02	57.23	84.56
$R_r$ (%)	99.44	100	98.81	97.21	99.9	100	100	100

Laminates have quite different behaviours because of the opposite effect of the number of CFR plies and the SMP interlayer. It is expected that loads increase by increasing the number of plies at constant SMP interlayer thickness, and this trend is generally confirmed. In particular, the frozen load ( $L_M$ ) always increases with the number of plies for all the maximum strains. The residual load, instead, partially reduces for the highest number of plies. In fact, CFR plies minimally participate to the SMP behaviour because of the small contribution from the epoxy matrix, whereas carbon fibres support laminate elasticity at all the temperatures. However, the role of the SMP interlayer is not univocal. By increasing its thickness, the CFR plies are separated and the stiffness increases but, in temperature, much more soft volume is present to allow fibre movements. As a result, the contribution of this higher softness may be stronger than the elastic contribution due to ply spacing. In fact, the  $L_R$  load for 8 ply laminate, and 300  $\mu\text{m}$  of SMP interlayer, is lower than the 6 ply with the same interlayer thickness. The difference is small but repetitive at all the strains.

The memory load is responsible for the shape recovery. Higher  $L_M$  loads lead to higher forces under constraints. It ranges between 0.31 N and 44.58 N, going from the thinnest to the thickest laminates. After normalisation, the comparison is more difficult because the SMP interlayer increases the stiffness but reduces the elastic modulus. In terms of shape recovery and fixity, all the laminates show good but not optimal ability of freezing the shape. The shape fixity is 65% on average, with a maximum about 80% for the 8 ply laminate with 300  $\mu\text{m}$  of SMP interlayer, and a minimum close to 50% for the same laminate with 100  $\mu\text{m}$  of interlayer. This fact shows the strong effect of the SMP interlayer thickness. By increasing this thickness, the SMPC laminate is less a structural composite and more a SMP material. Depending on the application, the designer can tailor the best material

performances. In all the cases, very high shape recovery values were reached, with an average of 98% and a minimum about 90%.

Results from durability tests are reported in Table 4, in analogy with Table 3.

**Table 4.** SM data from multiple cycling.

100 $\mu\text{m}$ SMP	2 Plies	4 Plies	6 Plies	8 Plies
$L_R$ (N)	$0.28 \pm 0.01$	$1.17 \pm 0.13$	$1.4 \pm 0.1$	$3.59 \pm 0.88$
$L_M$ (N)	$0.79 \pm 0.02$	$5.18 \pm 0.09$	$12.23 \pm 0.74$	$39.2 \pm 1.9$
$\sigma_R$ (MPa)	$16.43 \pm 0.46$	$14.04 \pm 1.56$	$7.26 \pm 0.54$	$7.96 \pm 1.95$
$\sigma_M$ (MPa)	$46.26 \pm 1.24$	$62.31 \pm 1.06$	$63.52 \pm 3.85$	$86.83 \pm 4.22$
300 $\mu\text{m}$ SMP	2 Plies	4 Plies	6 Plies	8 Plies
$L_R$ (N)	$0.31 \pm 0.02$	$1.24 \pm 0.21$	$2.2 \pm 0.1$	$2.0 \pm 0.7$
$L_M$ (N)	$2.28 \pm 0.03$	$12.72 \pm 0.71$	$19.97 \pm 1.64$	$27.86 \pm 5.33$
$\sigma_R$ (MPa)	$8.40 \pm 0.53$	$6.83 \pm 1.17$	$4.36 \pm 0.21$	$2.3 \pm 0.8$
$\sigma_M$ (MPa)	$62.44 \pm 0.44$	$70.22 \pm 3.93$	$40.2 \pm 3.3$	$34.19 \pm 6.55$

Due to the similarity of the repeated cycles, reference loads and stresses are reported as average and dispersion of the 10 cycles. Average values of  $L_M$  and  $L_R$  are slightly higher than those from single cycles because of the higher test rate. SM properties remain almost unaltered during cycling, the memory load has a dispersion between 2% and 6%. Higher scattering is found for the residual load because of the low value. In fact,  $L_R$  is on average 15% of  $L_M$ .

## 5. Conclusions

In this study, durability tests have been performed on SMPC laminates with different structure at low cycles. All the laminates answered in optimal way and showed a unique behaviour in terms of SM performances. In all the cases, delamination and cracks were avoided. In fact, SMPC laminates are always tested in their elastic range during the thermo-mechanical cycles. In the case of the single laminate under testing, the difference in the exerted loads depends on the reduction of the mechanical stiffness because of the temperature. Stresses arise due to polymer stretching in the memory step. If the failure limits are not overcome and degradation conditions are far, very high durability is expected. Experimental results confirm this assumption. In fact, fatigue phenomena cannot be discussed after 10 cycles, as in the current experimentation. Nevertheless, the good repeatability at low cycling is already sufficient for a lot of uses, above all for self-deploying structures in space. Even if the effect of the laminate structure can influence the comparison of the SM behaviour, provided data are available for possible use in designing of this kind of structures. By changing the number of plies of the SMPC as well as the SMP interlayer thickness, it is possible to find the optimal combination between structural and functional performances. Very high memory loads have been reached in the case of thick laminates, up to 45 N. Thinner laminates may be preferred in the case that high shape fixity is necessary. Shape recovery is already very high for all the laminates, independently from the applied strain.

**Author Contributions:** Conceptualisation, F.Q. and L.I.; Methodology, D.B., L.S. and L.I.; Validation, F.Q., L.I. and D.B.; Formal analysis, F.Q. and L.S.; Investigation, L.I.; Resources, F.Q. and L.S.; Data curation, L.I. and D.B.; Writing—original draft and review, F.Q.; Visualisation, L.I.; Supervision, L.S. and D.B.; Funding acquisition, F.Q. All authors have read and agreed to the published version of the manuscript.

**Funding:** This research was funded by the EU H2020 Project “Smart by Design and Intelligent by Architecture for turbine blade fan and structural components systems” (SMARTFAN) under Grant Agreement No. 760779.

**Data Availability Statement:** The data that support the findings of this study are available upon reasonable request from the authors.

**Acknowledgments:** The authors are grateful to Fabrizio Betti for the support given in the experimentation.

**Conflicts of Interest:** The authors declare no conflict of interest. The funders had no role in the design of the study; in the collection, analysis, or interpretation of data; in the writing of the manuscript, or in the decision to publish the results.

## References

1. Guo, J.; Lv, H.; Wang, Z.; Tang, X.; Liang, W.; Zhang, S. A Review of Shape Memory Polymers and Composites: Mechanisms, Materials, and Applications. *Adv. Mater.* **2020**, *33*, e2000713. [[CrossRef](#)]
2. Yu, Z.; Wang, Z.; Li, H.; Teng, J.; Xu, L. Shape memory epoxy polymer (SMEP) composite mechanical properties enhanced by introducing graphene oxide (GO) into the matrix. *Materials* **2019**, *12*, 1107. [[CrossRef](#)] [[PubMed](#)]
3. Peng, K.; Zhao, Y.; Shahab, S.; Mirzaeifar, R. Ductile Shape-Memory Polymer Composite with Enhanced Shape Recovery Ability. *ACS Appl. Mater. Interfaces* **2020**, *12*, 58295–58300. [[CrossRef](#)] [[PubMed](#)]
4. Santo, L.; Quadrini, F.; Ganga, P.L.; Zolesi, V. Mission BION-M1: Results of Ribes/Foam2 experiment on shape memory polymer foams and composites. *Aerosp. Sci. Technol.* **2015**, *40*, 109–114. [[CrossRef](#)]
5. Ameduri, S.; Ciminello, M.; Concilio, A.; Quadrini, F.; Santo, L. Shape Memory Polymer Composite Actuator: Modelling Approach for Preliminary Design and Validation. *Actuators* **2019**, *8*, 51. [[CrossRef](#)]
6. Santo, L.; Quadrini, F.; Accettura, A.G.; Villadei, W. Shape memory composites for self-deployable structures in aerospace applications. *Procedia Eng.* **2014**, *88C*, 42–47. [[CrossRef](#)]
7. Santo, L.; Quadrini, F.; Bellisario, D. Shape memory composite antennas for space applications. *IOP Conf. Ser.-Mat. Sci.* **2016**, *161*, 012066. [[CrossRef](#)]
8. Santo, L.; Bellisario, D.; Iorio, L.; Quadrini, F. Shape memory composite structures for self-deployable solar sails. *Astrodynamic* **2019**, *3*, 247–255. [[CrossRef](#)]
9. Quadrini, F.; Bellisario, D.; Iorio, L.; Santo, L. Shape memory polymer composites by molding aeronautical prepregs with shape memory polymer interlayers. *Mater. Res. Express* **2019**, *6*, 115711. [[CrossRef](#)]
10. Pretsch, T. Review on the Functional Determinants and Durability of Shape Memory Polymers. *Polymers* **2010**, *2*, 120–158. [[CrossRef](#)]
11. Tandon, G.P.; Goecke, K.; Cable, K.; Baur, J. Environmental durability of fabric-reinforced shape-memory polymer composites. *J. Intell. Mater. Syst. Struct.* **2010**, *21*, 1365–1381. [[CrossRef](#)]
12. Guo, J.; Wang, Z.; Tong, L.; Lv, H.; Liang, W. Shape memory and thermo-mechanical properties of shape memory polymer/carbon fiber composites. *Compos. Part A Appl. Sci. Manuf.* **2015**, *76*, 162–171. [[CrossRef](#)]
13. Guo, J.; Lv, H.; Wang, Z.; Tang, X.; Liang, W.; Zhang, S. Thermo-mechanical property of shape memory polymer/carbon fibre composites. *Mater. Res. Innov.* **2015**, *19*, 566–572. [[CrossRef](#)]
14. Gong, X.; Liu, L.; Liu, Y.; Leng, J. An electrical-heating and self-sensing shape memory polymer composite incorporated with carbon fiber felt. *Smart Mater. Struct.* **2016**, *25*, 035036. [[CrossRef](#)]
15. Li, F.; Scarpa, F.; Lan, X.; Liu, L.; Liu, Y.; Leng, J. Bending shape recovery of unidirectional carbon fiber reinforced epoxy-based shape memory polymer composites. *Compos. Part A Appl. Sci. Manuf.* **2019**, *116*, 169–179. [[CrossRef](#)]
16. Jang, J.H.; Hong, S.B.; Kim, J.G.; Goo, N.S.; Lee, H.; Yu, W.R. Long-term properties of carbon fiber-reinforced shape memory epoxy/polymer composites exposed to vacuum and ultraviolet radiation. *Smart Mater. Struct.* **2019**, *28*, 115013. [[CrossRef](#)]
17. Ren, Z.; Liu, L.; Liu, Y.; Leng, J. Damage and failure in carbon fiber-reinforced epoxy filament-wound shape memory polymer composite tubes under compression loading. *Polym. Test.* **2020**, *85*, 106387. [[CrossRef](#)]
18. Margoy, D.; Gouzman, I.; Grossman, E.; Bolker, A.; Eliaz, N.; Verker, R. Epoxy-based shape memory composite for space applications. *Acta Astronaut.* **2021**, *178*, 908–919. [[CrossRef](#)]
19. Quadrini, F.; Santo, L.; Squeo, A. Shape memory epoxy foams for space applications. *Mater. Lett.* **2012**, *69*, 20–23.
20. Santo, L.; Bellisario, D.; Quadrini, F. Shape memory behavior of PET foams. *Polymers* **2018**, *10*, 115. [[CrossRef](#)]
21. Tedde, G.M.; Santo, L.; Bellisario, D.; Iorio, L.; Quadrini, F. Frozen Stresses in shape memory polymer composites. *Mater. Plast.* **2018**, *55*, 494–497. [[CrossRef](#)]